Electronic excitations in correlated finite 2D materials generated by ion impact

Niclas Schlünzen, Jan-Philip Joost, Karsten Balzer, Lotte Borkowski, Hannes Ohldag, and Michael Bonitz

C A U
Christian-Albrechts-Universität zu Kiel
Mathematisch-Naturwissenschaftliche Fakultät

APS March Meeting
March 2022, online

detailed version of talk at:
www.theo-physik.uni-kiel.de/bonitz/talks.html

Christian-Albrechts-Universität zu Kiel
Mathematisch-Naturwissenschaftliche Fakultät

Fermionic atoms in optical lattices
tunable lattice depth and interaction

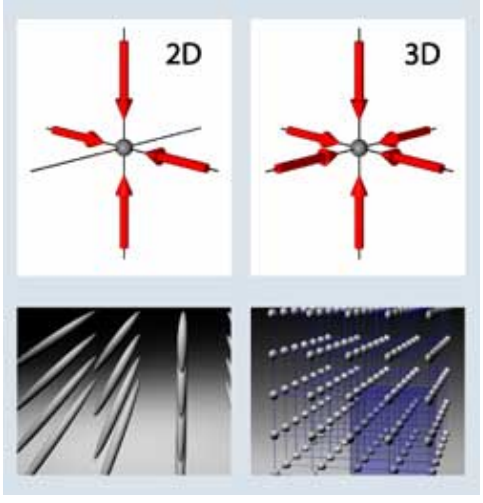

Fig.: M. Greiner (Harvard)

Graphene: high mobility, no bandgap

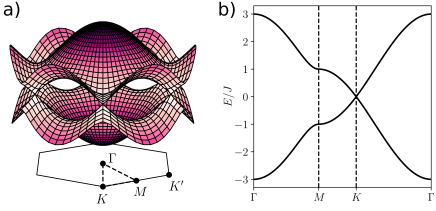

Graphene nanoribbons:
finite tunable bandgap

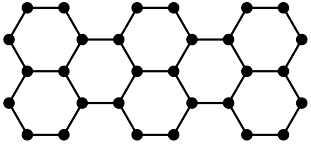

GNR: spatially localized spectral contributions

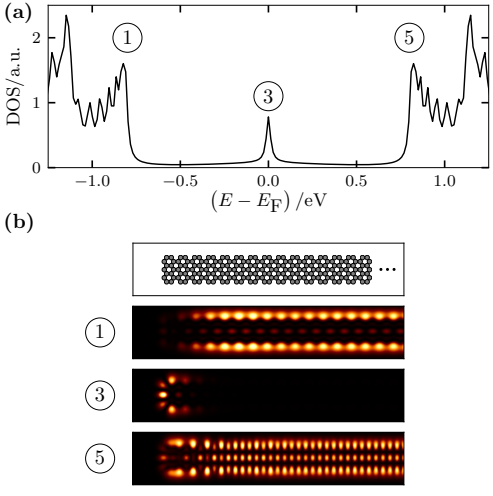

7 armchair GNR of 504 atoms, GW-NEGF ground state simulation, J.-P. Joost, A.-P. Jauho, and M. Bonitz, Nano Letters (2019)

- top: total density of states (DOS)
- DOS size and shape dependent
- importance of e-e interactions
- topological states, strong Coulomb correlations

Consider nonequilibrium electron dynamics following ion impact

$\Rightarrow$ very strong localized excitation

$\Rightarrow$ energy gain, charge transfer

$\Rightarrow$ creation of doublons[a]

$\Rightarrow$ ions sensitive non-destructive local diagnostic of electronic properties

[a] K. Balzer et al., PRL (2018)

The extreme case: Stopping of highly charged ions in 2D materials[1]

ABSTRACT: Low-energy electrons (LEEs) are of great relevance for ion-induced radiation damage in cells and genes. We show that charge exchange of ions leads to LEE emission upon impact on condensed matter. By using a graphene monolayer as a simple model system for condensed organic matter and utilizing slow highly charged ions (HCIs) as projectiles, we highlight the importance of charge exchange alone for LEE emission. We find a large number of ejected electrons resulting from individual ion impacts (up to 80 electrons/ion for Xe^{40+}). More than 90% of emitted electrons have energies well below 15 eV. This "splash" of low-energy electrons is interpreted as the consequence of ion deexcitation via an interatomic Coulombic decay (ICD) process.

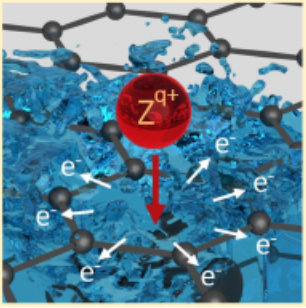

- ultrafast electronic processes (1...5 fs)
- strong excitation: nonlinear and non-adiabatic response
- rapid intralayer electron transport
- emission of low-energy electrons, strong dependence on target properties

⇒ Needed: nonequilibrium quantum many-body theory for inhomogeneous systems

[1] Schwestka *et al.*, J. Phys. Chem. Lett. **10**, 4805 (2019)

C | A | U
Christian-Albrechts-Universität zu Kiel
Mathematisch-Naturwissenschaftliche Fakultät

2nd quantization

- Fock space $\mathcal{F} \ni |n_1, n_2 \ldots\rangle$, $\quad \mathcal{F} = \bigoplus_{N_0 \in \mathbb{N}} \mathcal{F}^{N_0}$, $\quad \mathcal{F}^{N_0} \subset \mathcal{H}^{N_0}$
- $\hat{c}_i$,$\hat{c}_i^\dagger$ creates/annihilates a particle in single-particle orbital ϕ_i
- spin accounted for by canonical (anti-)commutator relations
  $\left[\hat{c}_i^{(\dagger)}, \hat{c}_j^{(\dagger)}\right]_\mp = 0, \quad \left[\hat{c}_i, \hat{c}_j^\dagger\right]_\mp = \delta_{i,j}$
- Hamiltonian: $\hat{H}(t) = \underbrace{\sum_{k,m} h^0_{km} \hat{c}_k^\dagger \hat{c}_m}_{\hat{H}_0} + \underbrace{\frac{1}{2} \sum_{k,l,m,n} w_{klmn}\, \hat{c}_k^\dagger \hat{c}_l^\dagger \hat{c}_n \hat{c}_m}_{\hat{W}} + \hat{F}(t)$

Particle interaction w_{klmn}

- Coulomb interaction
- electronic correlations

Time-dependent excitation $\hat{F}(t)$

- single-particle type
- em field, quench, particles

C | A | U
Christian-Albrechts-Universität zu Kiel
Mathematisch-Naturwissenschaftliche Fakultät

two times $z, z' \in \mathcal{C}$ ("Keldysh contour"), arbitrary one-particle basis $|\phi_i\rangle$

$$\boxed{G_{ij}(z,z') = \tfrac{\mathrm{i}}{\hbar}\left\langle \hat{T}_{\mathcal{C}} \hat{c}_i(z) \hat{c}_j^\dagger(z') \right\rangle}$$

average with $\hat{\rho}_N$

pure or mixed state

Keldysh–Kadanoff–Baym equations (KBE) on $\mathcal{C}$ (2×2 matrix):

$$\sum_k \left\{ \mathrm{i}\hbar \frac{\partial}{\partial z} \delta_{ik} - h_{ik}(z) \right\} G_{kj}(z,z') = \delta_{\mathcal{C}}(z,z')\delta_{ij} - \mathrm{i}\hbar \sum_{klm} \int_{\mathcal{C}} \mathrm{d}\bar{z}\, w_{iklm}(z^+,\bar{z}) G^{(2)}_{lmjk}(z,\bar{z};z',\bar{z}^+)$$

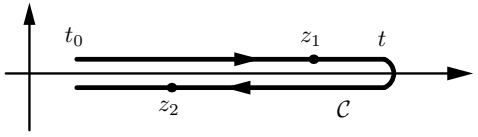

KBE: first equation of Martin–Schwinger hierarchy for $G, G^{(2)} \ldots G^{(n)}$

- $\int_{\mathcal{C}} wG^{(2)} \to \int_{\mathcal{C}} \Sigma G$, Selfenergy
- Nonequilibrium Diagram technique
  Example: Hartree–Fock + Second Born selfenergy

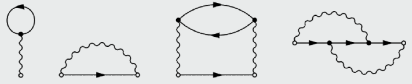

Real-Time Keldysh–Kadanoff–Baym Equations (KBE)

- Correlation functions $G^{\gtrless}$ obey real-time KBE

$$\sum_l \left[\mathrm{i}\hbar \frac{\mathrm{d}}{\mathrm{d}t} \delta_{i,l} - h^{\mathrm{eff}}_{il}(t) \right] G^{>}_{lj}(t,t') = I^{(1),>}_{ij}(t,t') \,,$$

$$\sum_l G^{<}_{il}(t,t') \left[-\mathrm{i}\hbar \frac{\overleftarrow{\mathrm{d}}}{\mathrm{d}t'} \delta_{l,j} - h^{\mathrm{eff}}_{lj}(t') \right] = I^{(2),<}_{ij}(t,t') \,,$$

with the effective single-particle **Hartree–Fock Hamiltonian**

$$h^{\mathrm{eff}}_{ij}(t) = h^{0}_{ij} \pm \mathrm{i}\hbar \sum_{kl} w^{\pm}_{ikjl} G^{<}_{lk}(t)$$

and the collision integrals

$$I^{(1),>}_{ij}(t,t') \coloneqq \sum_l \int_{t_\mathrm{s}}^{\infty} \mathrm{d}\bar{t} \left\{ \Sigma^{\mathrm{R}}_{il}(t,\bar{t}) G^{>}_{lj}(\bar{t},t') + \Sigma^{>}_{il}(t,\bar{t}) G^{\mathrm{A}}_{lj}(\bar{t},t') \right\},$$

$$I^{(2),<}_{ij}(t,t') \coloneqq \sum_l \int_{t_\mathrm{s}}^{\infty} \mathrm{d}\bar{t} \left\{ G^{\mathrm{R}}_{il}(t,\bar{t}) \Sigma^{<}_{lj}(\bar{t},t') + G^{<}_{il}(t,\bar{t}) \Sigma^{\mathrm{A}}_{lj}(\bar{t},t') \right\}.$$

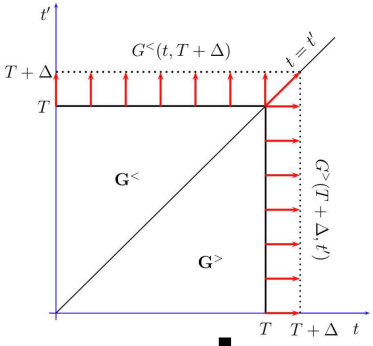

$$\mathcal{O}(N_\mathrm{t}^3)$$

- numerically demanding due to N_t^3 scaling (most competing methods time linear)

Christian-Albrechts-Universität zu Kiel
Mathematisch-Naturwissenschaftliche Fakultät

Full two-time solutions: Danielewicz, Schäfer, Köhler/Kwong, Bonitz/Semkat, Haug, Jahnke, van Leeuwen, Stefanucci, Verdozzi, Berges, Garny ...

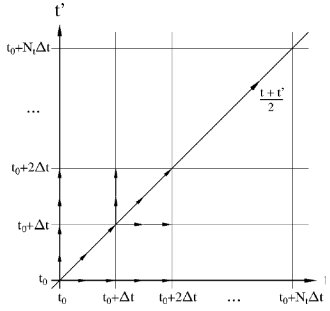

1. adiabatically slow switch-on of interaction for $t, t' \leq t_0$ [1-3]

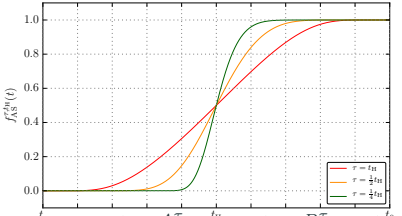

$$f_{\rm AS}^{\tau,t_{\rm H}}(t) = \exp\left(-\frac{A_{t_{\rm H}}^{\tau}}{t/(2t_{\rm H})}t \exp\left(\frac{B_{t_{\rm H}}^{\tau}}{t/(2t_{\rm H})-1}\right)\right)$$

$$B_{t_{\rm H}}^{\tau} := \frac{t_{\rm H}}{\tau \ln(2)} - \frac{1}{2}, \quad A_{t_{\rm H}}^{\tau} := \frac{\ln(2)}{2} \mathrm{e}^{2B_{t_{\rm H}}^{\tau}}$$

2. solve KBE in $t - t'$ plane for $G^{\gtrless}(t, t')$ with same code

[1] A. Rios et al., Ann. Phys. **326**, 1274 (2011), [2] S. Hermanns et al., Phys. Scr. **T151**, 014036 (2012)
[3] M. Watanabe and W. P. Reinhardt, Phys. Rev. Lett. **65**, 3301 (1990)

Nonequilibrium selfenergy approximations[2]

Hartree–Fock (HF, mean field): $\sim w^1$

Second Born (2B): $\sim w^2$

GW: ∞ bubble summation, dynamical screening effects

particle-particle T-matrix (TPP): ∞ ladder sum in pp channel

particle-hole T-matrix (TPH/TEH): ∞ ladder sum in ph channel

3rd order approx. (TOA): $\sim w^3$

dynamically screened ladder (DSL): includes GW and $\mathrm{TPP} + \mathrm{TPH}$ diagrams

Choice depends on coupling strength, density (filling)

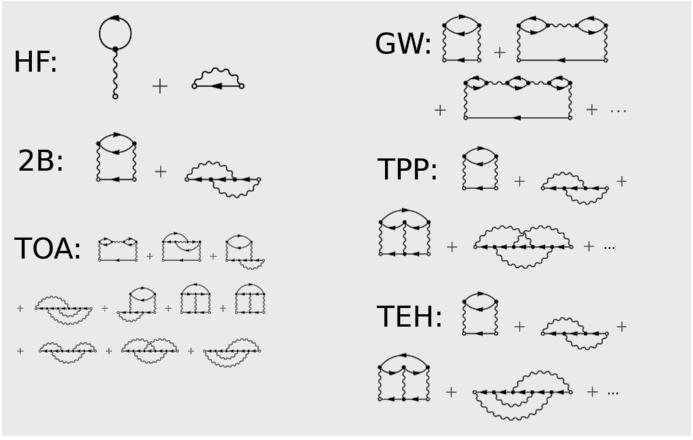

[2]Conserving approximations, two-time functions $\Sigma(t, t')$, applies for ultra-short to long times
Review: Schlünzen *et al.*, J. Phys. Cond. Matt. **32**, 103001 (2020)
DSL – details and benchmarks: Joost *et al.*, submitted for publication, arXiv:2202.10061

Acceleration: Generalized Kadanoff–Baym Ansatz (GKBA)[3]

- full propagation on the time diagonal ($I \coloneqq I^{(1),<}$):

$$\mathrm{i}\hbar\frac{\mathrm{d}}{\mathrm{d}t}G^<_{ij}(t) = \left[h^{\mathrm{HF}}, G^<\right]_{ij}(t) + \left[I + I^\dagger\right]_{ij}(t)$$

- reconstruct off-diagonal NEGF from time diagonal:

$$G^{\gtrless}_{ij}(t,t') = \pm\left[G^{\mathrm{R}}_{ik}(t,t')\rho^{\gtrless}_{kj}(t') - \rho^{\gtrless}_{ik}(t)G^{\mathrm{A}}_{kj}(t,t')\right]$$

with $\quad \rho^{\gtrless}_{ij}(t) = \pm\mathrm{i}\hbar G^{\gtrless}_{ij}(t,t)$

- HF-GKBA: use Hartree–Fock propagators for $G^{\mathrm{R/A}}_{ij}$

$$G^{\mathrm{R/A}}_{ij}(t,t') = \mp\mathrm{i}\Theta_{\mathcal{C}}\left(\pm[t-t']\right)\exp\left(-\frac{\mathrm{i}}{\hbar}\int_{t'}^{t}\mathrm{d}\bar{t}\, h_{\mathrm{HF}}(\bar{t})\right)\Big|_{ij}$$

- conserves total energy

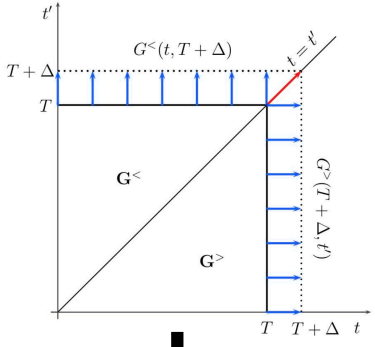

$$\mathcal{O}\left(N_{\mathrm{t}}^2\right)$$

[6] P. Lipavský, V. Špička, and B. Velický, Phys. Rev. B **34**, 6933 (1986);
K. Balzer and M. Bonitz, Lecture Notes in Physics **867** (2013)

HF-GKBA (SOA) results for materials, plasmas, atoms, molecules

C | A | U
Christian-Albrechts-Universität zu Kiel
Mathematisch-Naturwissenschaftliche Fakultät

2D Layered Materials

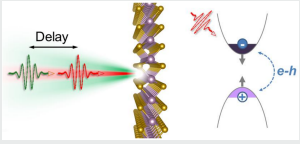

E. A. Pogna *et al.*,
ACS Nano **10**, 1182 (2016)

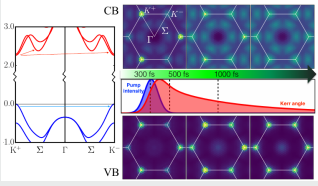

A. Molina-Sánchez *et al.*,
Nano Lett. **17**, 4549 (2017)

Ion Stopping in Hexagonal Lattices

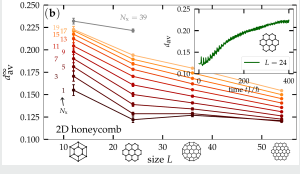

K. Balzer *et al.*,
PRL **121**, 267602 (2018)

Semiconductors

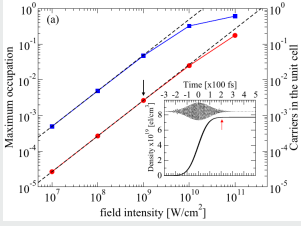

D. Sangalli *et al.*,
PRB **93**, 195205 (2016)

Laser-Induced Heating of Dense Plasmas

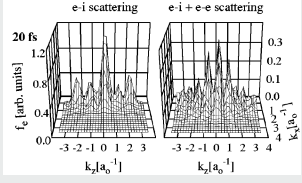

H. Haberland *et al.*,

PRE **64**, 026405 (2001)
gauge-invariant

multi-photon absorption

inv bremsstrahlung heating

Further results: Hermanns *et al.*, PRB 2014
Bonitz *et al.*, phys. stat. sol. (b) 2019
atoms, molecules: Stefanucci *et al.*

The G1–G2 Scheme: exact reformulation of HF-GKBA

[Schlünzen et al., Phys. Rev. Lett. 2020]

Christian-Albrechts-Universität zu Kiel
Mathematisch-Naturwissenschaftliche Fakultät

- full propagation on the time diagonal as for ordinary HF-GKBA:

$$\mathrm{i}\hbar\frac{\mathrm{d}}{\mathrm{d}t}G^{<}_{ij}(t) = \left[h^{\mathrm{HF}}, G^{<}\right]_{ij}(t) + \left[I + I^{\dagger}\right]_{ij}(t)$$

- but collision integral defined by correlated two-particle Green function

$$I_{ij}(t) = \pm\mathrm{i}\hbar\sum_{klp} w_{iklp}(t)\mathcal{G}_{lpjk}(t)$$

$\mathcal{O}(N_{\mathrm{t}}^1)$

- which obeys an ordinary differential equation[4]

$$\mathrm{i}\hbar\frac{\mathrm{d}}{\mathrm{d}t}\mathcal{G}_{ijkl}(t) = \left[h^{(2),\mathsf{HF}}, \mathcal{G}\right]_{ijkl}(t) + \Psi^{\pm}_{ijkl}(t)$$

- the initial values

$$G^{0,<}_{ij} = \pm\frac{1}{\mathrm{i}\hbar}n_{ij}(t_0) =: \pm\frac{1}{\mathrm{i}\hbar}n^0_{ij}\,,$$
$$\mathcal{G}^0_{ijkl} = \frac{1}{(\mathrm{i}\hbar)^2}\left\{n^0_{ijkl} - n^0_{ik}n^0_{jl} \mp n^0_{il}n^0_{jk}\right\}\,,$$

determine the density and the pair correlations existing in the system at the initial time $t = t_0$

[4] two-particle commutator: $[A, B]_{ijkl}(t) = \sum_{pq}\left[A_{ijpq}(t)B_{pqkl}(t) - B_{ijpq}(t)A_{pqkl}(t)\right]$

The G1–G2 Scheme: beyond 2nd Born selfenergy

- other selfenergy approximations can be reformulated in the G1–G2 scheme in similar fashion:[5]

$$\mathrm{i}\hbar\frac{\mathrm{d}}{\mathrm{d}t}\mathcal{G}_{ijkl}(t) = \Big[h^{(2),\mathsf{HF}}(t),\mathcal{G}(t)\Big]_{ijkl} + \Psi^{\pm}_{ijkl}(t) + \underbrace{L_{ijkl}(t)}_{\text{TPP}} + \underbrace{P_{ijkl}(t)}_{GW} \pm \underbrace{P_{jikl}(t)}_{\text{TPH}}$$

with (times dropped)

$$L_{ijkl} \coloneqq \sum_{pq}\left\{\mathfrak{h}^{L}_{ijpq}\mathcal{G}_{pqkl} - \mathcal{G}_{ijpq}\Big[\mathfrak{h}^{L}_{klpq}\Big]^{*}\right\}, \qquad \mathfrak{h}^{L}_{ijkl} \coloneqq (\mathrm{i}\hbar)^2\sum_{pq}\left[\mathcal{G}^{\mathsf{H},>}_{ijpq} - \mathcal{G}^{\mathsf{H},<}_{ijpq}\right] w_{pqkl}\,,$$

$$P_{ijkl} \coloneqq \sum_{pq}\left\{\mathfrak{h}^{\Pi}_{qjpl}\mathcal{G}_{piqk} - \mathcal{G}_{qjpl}\Big[\mathfrak{h}^{\Pi}_{qkpi}\Big]^{*}\right\}, \qquad \mathfrak{h}^{\Pi}_{ijkl} \coloneqq \pm(\mathrm{i}\hbar)^2\sum_{pq} w^{\pm}_{qipk}\left[\mathcal{G}^{\mathsf{F},>}_{jplq} - \mathcal{G}^{\mathsf{F},<}_{jplq}\right]$$

and the Hartree/Fock (H/F) two-particle Green functions

$$\mathcal{G}^{\mathsf{H},\gtrless}_{ijkl}(t) \coloneqq G^{\gtrless}_{ik}(t,t)G^{\gtrless}_{jl}(t,t)\,, \qquad \mathcal{G}^{\mathsf{F},\gtrless}_{ijkl}(t) \coloneqq G^{\gtrless}_{il}(t,t)G^{\lessgtr}_{jk}(t,t)$$

- including all terms results in the dynamically-screened-ladder (DSL) approximation

[5] J.-P. Joost, N. Schlünzen, and M. Bonitz, Phys. Rev. B **101**, 245101 (2020)

details on DSL: N. Schlünzen et al., submitted for publication, arXiv:2202.1061

Numerical Scaling of G1–G2 vs. Standard HF-GKBA

- linear time scaling outweights introduction of 4-dimensional two-particle Green function
  → new scheme an improvement in most cases of practical relevance

		Σ				
Basis	**HF-GKBA**	**2B**	***GW***	**TPP**	**TPH**	**DSL**
general	standard	$\mathcal{O}\left(N_\mathrm{b}^5 N_\mathrm{t}^2\right)$	$\mathcal{O}\left(N_\mathrm{b}^6 N_\mathrm{t}^3\right)$	$\mathcal{O}\left(N_\mathrm{b}^6 N_\mathrm{t}^3\right)$	$\mathcal{O}\left(N_\mathrm{b}^6 N_\mathrm{t}^3\right)$	–
	G1–G2	$\mathcal{O}\left(N_\mathrm{b}^5 N_\mathrm{t}^1\right)$	$\mathcal{O}\left(N_\mathrm{b}^6 N_\mathrm{t}^1\right)$	$\mathcal{O}\left(N_\mathrm{b}^6 N_\mathrm{t}^1\right)$	$\mathcal{O}\left(N_\mathrm{b}^6 N_\mathrm{t}^1\right)$	$\mathcal{O}\left(N_\mathrm{b}^6 N_\mathrm{t}^1\right)$
	speedup ratio	$\mathcal{O}\left(N_\mathrm{t}\right)$	$\mathcal{O}\left(N_\mathrm{t}^2\right)$	$\mathcal{O}\left(N_\mathrm{t}^2\right)$	$\mathcal{O}\left(N_\mathrm{t}^2\right)$	–
Hubbard	standard	$\mathcal{O}\left(N_\mathrm{b}^3 N_\mathrm{t}^2\right)$	$\mathcal{O}\left(N_\mathrm{b}^3 N_\mathrm{t}^3\right)$	$\mathcal{O}\left(N_\mathrm{b}^3 N_\mathrm{t}^3\right)$	$\mathcal{O}\left(N_\mathrm{b}^3 N_\mathrm{t}^3\right)$	–
	G1–G2	$\mathcal{O}\left(N_\mathrm{b}^4 N_\mathrm{t}^1\right)$	$\mathcal{O}\left(N_\mathrm{b}^4 N_\mathrm{t}^1\right)$	$\mathcal{O}\left(N_\mathrm{b}^4 N_\mathrm{t}^1\right)$	$\mathcal{O}\left(N_\mathrm{b}^4 N_\mathrm{t}^1\right)$	$\mathcal{O}\left(N_\mathrm{b}^4 N_\mathrm{t}^1\right)$
	speedup ratio	$\mathcal{O}\left(N_\mathrm{t}/N_\mathrm{b}\right)$	$\mathcal{O}\left(N_\mathrm{t}^2/N_\mathrm{b}\right)$	$\mathcal{O}\left(N_\mathrm{t}^2/N_\mathrm{b}\right)$	$\mathcal{O}\left(N_\mathrm{t}^2/N_\mathrm{b}\right)$	–
HEG	standard	$\mathcal{O}\left(N_\mathrm{b}^3 N_\mathrm{t}^2\right)$	$\mathcal{O}\left(N_\mathrm{b}^3 N_\mathrm{t}^3\right)$	$\mathcal{O}\left(N_\mathrm{b}^3 N_\mathrm{t}^3\right)$	$\mathcal{O}\left(N_\mathrm{b}^3 N_\mathrm{t}^3\right)$	–
	G1–G2	$\mathcal{O}\left(N_\mathrm{b}^3 N_\mathrm{t}^1\right)$	$\mathcal{O}\left(N_\mathrm{b}^3 N_\mathrm{t}^1\right)$	$\mathcal{O}\left(N_\mathrm{b}^4 N_\mathrm{t}^1\right)$	$\mathcal{O}\left(N_\mathrm{b}^4 N_\mathrm{t}^1\right)$	$\mathcal{O}\left(N_\mathrm{b}^4 N_\mathrm{t}^1\right)$
	speedup ratio	$\mathcal{O}\left(N_\mathrm{t}\right)$	$\mathcal{O}\left(N_\mathrm{t}^2\right)$	$\mathcal{O}\left(N_\mathrm{t}^2/N_\mathrm{b}\right)$	$\mathcal{O}\left(N_\mathrm{t}^2/N_\mathrm{b}\right)$	–

Numerical Scaling of G1–G2 vs. Standard HF-GKBA

- time-linear scaling illustrated for the 10-site Hubbard chain

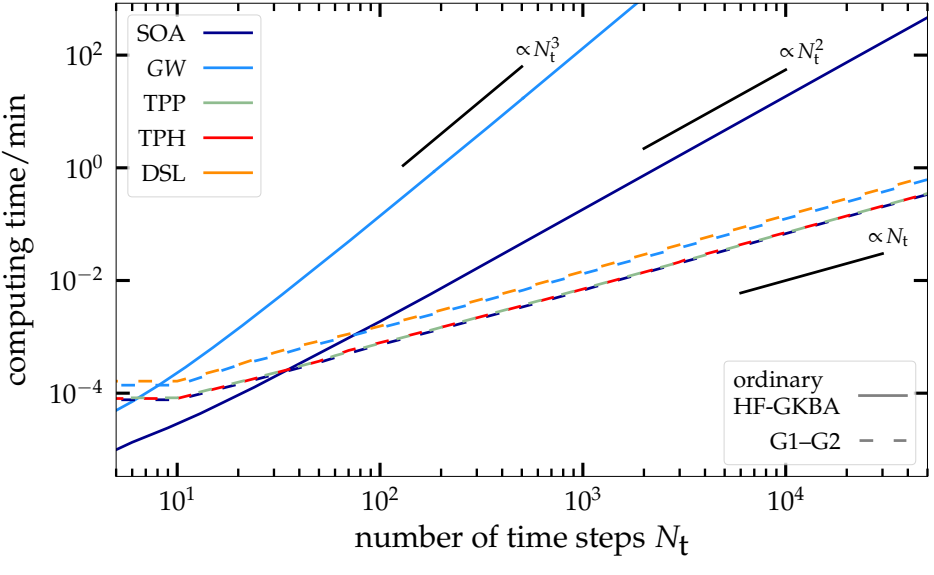

Modeling correlated electrons in 2D materials: Hubbard model

- Single band, small bandwidth, input from electronic structure calculations
- straightforward extension: multiple bands, long range interaction etc.

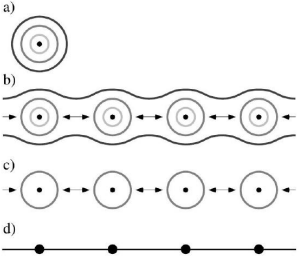

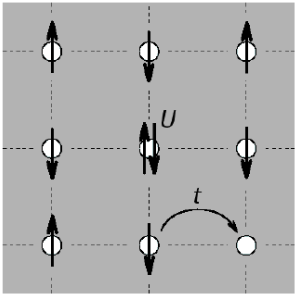

$$\hat{H}(t) = J \sum_{ij,\,\alpha} h_{ij}\, \hat{c}^{\dagger}_{i\alpha} \hat{c}_{j\alpha} + U \sum_i \hat{c}^{\dagger}_{i\uparrow} \hat{c}_{i\uparrow} \hat{c}^{\dagger}_{i\downarrow} \hat{c}_{i\downarrow} + \sum_{ij,\alpha\beta} f_{ij,\alpha\beta}(t)\, \hat{c}^{\dagger}_{i\alpha} \hat{c}_{j\beta}$$

$h_{ij} = -\delta_{\langle i,\,j\rangle}$ and $\delta_{\langle i,\,j\rangle} = 1$, if (i,j) is nearest neighbor, $\delta_{\langle i,\,j\rangle} = 0$ otherwise
use $J = 1$, on-site repulsion $(U > 0)$ or attraction $(U < 0)$
f: external time-dependent excitation
Example ion impact: $f(t) \sim \sum_i -\frac{Z(t) e_0^2}{|\mathbf{R}(t) - \mathbf{r}_i|}$, NEGF-Ehrenfest approach

NEGF-Ehrenfest simulations of ion stopping: ion energy loss

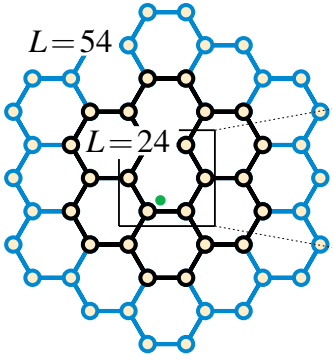

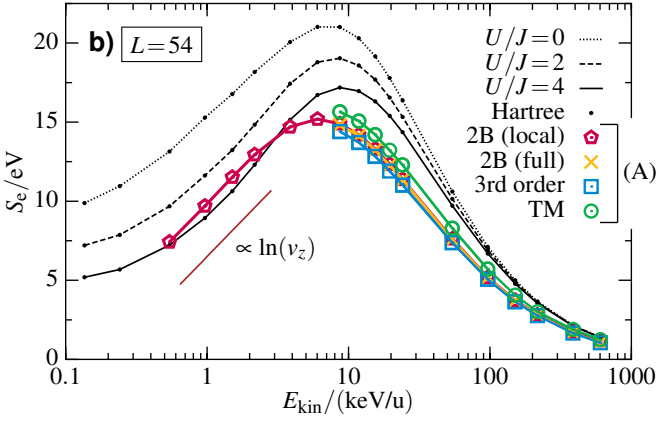

Left: finite honeycomb cluster and impact point of ion (green). Right: Ion energy loss S_e vs. impact energy. Black lines: Hartree approximation for e-e interaction. Colors: different approximations for the correlation selfenergy. From: Balzer *et al.* PRB (2016)

Density and doublon number dynamics during ion impact

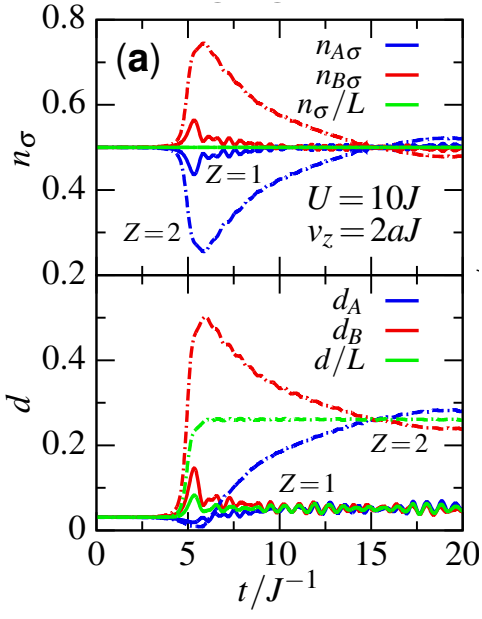

Top: electron density dynamics during ion impact ($t = 6$). Full (dash-dotted) lines: proton (α-particle). n_A: honeycomb ring closest to impact point. n_B second nearest ring. Green lines: mean density

Bottom: d_A (d_B): doublon number at nearest (second nearest) honeycomb ring.
$\Rightarrow$ increased doublon number remains in cluster after impact. Spreads uniformly across cluster.

From: Balzer *et al.* PRL (2018)

Doublon production by multiple ion impacts

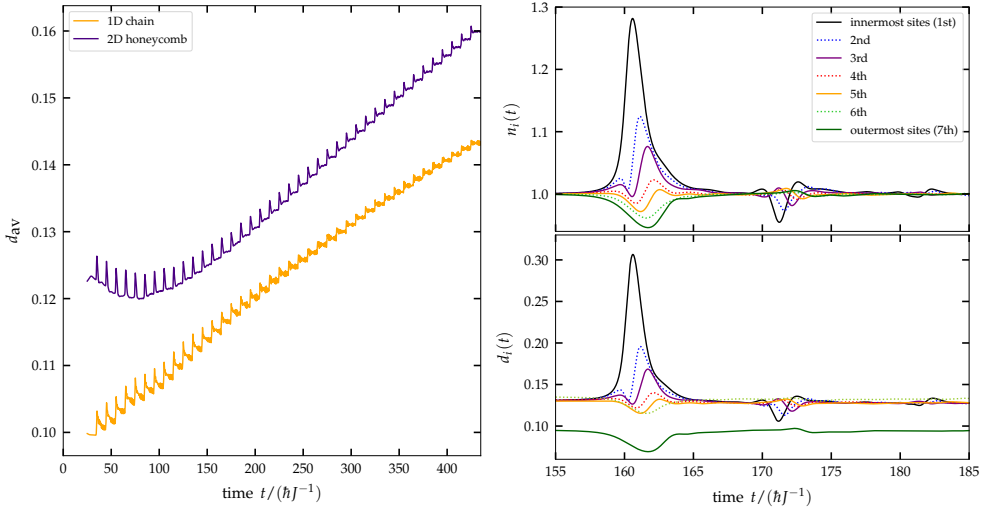

Left: dynamics of total doublon number upon up to 40 ion impacts for a 1D chain and 2D cluster with 96 sites. Right: site resolved density dynamics. From: Borkowski *et al.* phys. stats. sol. (b) (2022), https://doi.org/10.1002/pssb.202100511. Follow up of Balzer *et al.*, PRL **121**, 267602 (2018)

Ion impact induced change of photoemission signal (DOS)

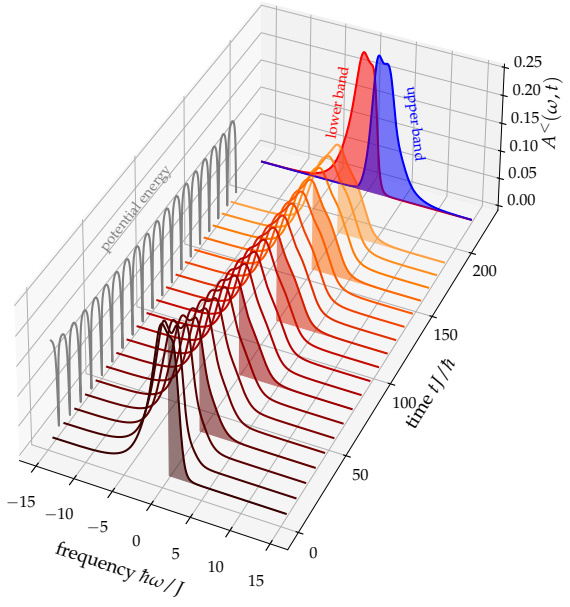

Time evolution of the photoemission spectrum (spectral function $A^<$) during 20 ion impacts, honeycomb, $L = 12$ with $U/J = 4$.
Occupation of upper Hubbard band (positive energies) increases with time.
Red (blue): (un)occupied states of un-excited system.
$t_0 = \hbar/J \approx 0.17$fs, $a_0 = 1.42$,
$v_0 = a_0/t_0 \approx 0.8 \cdot 10^6$m/s

from Bonitz *et al.* phys. stats. sol. (b) **257**, 1800490 (2019)

C|A|U
Christian-Albrechts-Universität zu Kiel
Mathematisch-Naturwissenschaftliche Fakultät

Summary

- Results for ion stopping in 2D graphene or TMDC monolayers
- potentially highly sensitive diagnostic of electronic correlation effects
- Nonequilibrium Green functions–Ehrenfest approach
- efficient time propagation using the G1–G2 scheme[6]
- generation and propagation of doublons via multiple ion impacts[7]
- ion neutralization treated via embedding selfenergy approach, see appendix[8]

Outlook

- Extension to bilayers and TMDCs
- Quantum treatment of electron dynamics in ion
- Impact of highly charged ions gives rise to electron emission (Auger, ICD). Electron number highly sensitive to electron mobility[9]

detailed version of talk at: www.theo-physik.uni-kiel.de/bonitz/talks.html

[6] Schlünzen *et al.*, Phys. Rev. Lett. 2020
[7] Balzer *et al.*, Phys. Rev. Lett. 2018; Borkowski *et al.*, phys. stat. sol. (b) (2022)
[8] Balzer and Bonitz, Contrib. Plasma Phys. **62** (2) e202100041 (2022)
[9] A. Niggas *et al.*, submitted for publication

Appendix: NEGF-embedding scheme for charge transfer from graphene nanoflake to impacting high Z ion

C | A | U
Christian-Albrechts-Universität zu Kiel
Mathematisch-Naturwissenschaftliche Fakultät

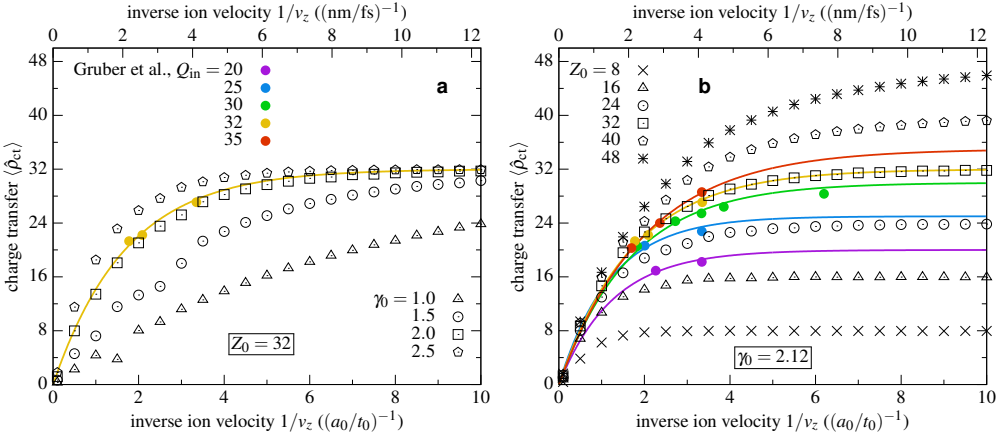

NEGF-embedding selfenergy scheme for resonant charge transfer, $L = 24$. Exp. data from Gruber et al. Nat. Commun. 2016, **7**(1), 13948. Single adjustable parameter γ_0 works for all charges. Figure from Balzer and Bonitz, Contrib. Plasma Phys. **62** (2) e202100041 (2022)

Charge transfer from graphene nanoflake to impacting high Z ion

C | A | U
Christian-Albrechts-Universität zu Kiel
Mathematisch-Naturwissenschaftliche Fakultät

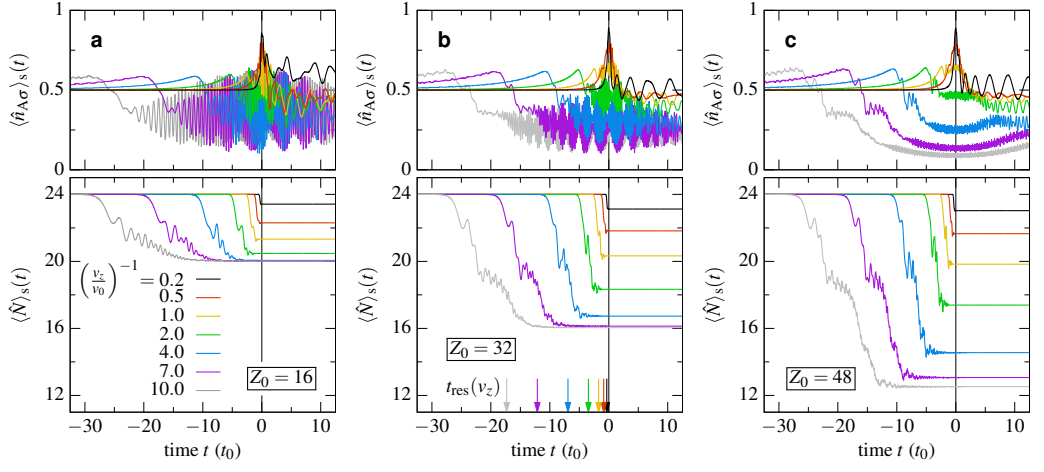

Dynamics of total particle number $\langle \hat{N} \rangle_s$ (in one band) and occupation $\langle \hat{n}_{0\sigma} \rangle_s$ of innermost honeycomb (graphene, $L = 24$ sites) during ion impact. Colors: NEGF results for different ion velocities. Arrows: moment when ion passes through the resonance point $z_{res} = \sqrt{3} a_0$, in front of the plane.
From Balzer and Bonitz, Contrib. Plasma Phys. **62** (2) e202100041 (2022). New results: electron emission into vacuum (ICD), graphene vs. MoS_2, A. Niggas et al., subm. for publication